

High-resolution measurements of the thermal expansion of superconducting Co-doped BaFe<sub>2</sub>As<sub>2</sub>M. S. da Luz,<sup>1</sup> J. J. Neumeier,<sup>1</sup> R. K. Bollinger,<sup>1</sup> A. S. Sefat,<sup>2</sup> M. A. McGuire,<sup>2</sup> R. Jin,<sup>2</sup> B. C. Sales,<sup>2</sup> and D. Mandrus<sup>2</sup><sup>1</sup>Department of Physics, Montana State University, Bozeman, P.O. Box 173840, Montana 59717-3840, USA<sup>2</sup>Materials Science and Technology Division, Oak Ridge National Laboratory, Oak Ridge, Tennessee 37831, USA

(Received 10 April 2009; revised manuscript received 15 May 2009; published 4 June 2009)

High-resolution thermal expansion measurements of single crystalline BaFe<sub>1.84</sub>Co<sub>0.16</sub>As<sub>2</sub> and BaFe<sub>1.77</sub>Co<sub>0.23</sub>As<sub>2</sub> in the temperature range  $5 < T < 300$  K are reported. The thermal expansion is highly anisotropic, with the largest expansion along the  $c$  axis. Distinct anomalies are present at the normal-to-superconducting phase-transition temperature  $T_c$ ; the phase transition appears to be continuous. No structural transitions are observed over the temperature range of our measurements. The thermal expansion data and heat-capacity data acquired on the same specimens are used to estimate the volumetric pressure derivative of  $T_c$  using the Ehrenfest relation.

DOI: 10.1103/PhysRevB.79.214505

PACS number(s): 74.25.Bt, 65.40.De, 65.40.Ba

The newly discovered iron-based layered superconductors include the 1111 family,  $R\text{FeAsO}_{1-x}\text{F}_x$  ( $R=\text{La, Nd, and Sm}$ ) with superconducting transition temperatures<sup>1</sup>  $T_c$  as high as 54 K and the related 122 family,  $A\text{Fe}_2\text{As}_2$  ( $A=\text{Ca, Sr, Ba, and Eu}$ ), which superconduct after doping<sup>2-5</sup> or under quasi-hydrostatic pressure.<sup>6-9</sup> Within the 122 family, CaFe<sub>2</sub>As<sub>2</sub>, SrFe<sub>2</sub>As<sub>2</sub>, BaFe<sub>2</sub>As<sub>2</sub>, and EuFe<sub>2</sub>As<sub>2</sub> exhibit a structural phase transition from a high-temperature tetragonal phase to orthorhombic at temperatures of 170, 203, 140, and 190 K respectively.<sup>9-11</sup> In the case of CaFe<sub>2</sub>As<sub>2</sub>, pressure suppresses the phase transition. If the pressure is quasihydrostatic, superconductivity occurs.<sup>7</sup> If the pressure is hydrostatic, a new low-temperature tetragonal phase forms, called the collapsed tetragonal phase; this phase does not superconduct.<sup>9</sup> Nonetheless, stabilization of the tetragonal phase appears to be a prerequisite for superconductivity.<sup>2,5</sup> Cobalt doping manages this while also adding carriers to the FeAs layers, leading to superconductivity<sup>5</sup> at 22 K in BaFe<sub>1.8</sub>Co<sub>0.2</sub>As<sub>2</sub>.

In this paper, we present thermal expansion and heat-capacity measurements of two compositions of superconducting Ba(Fe<sub>1-x</sub>Co<sub>x</sub>)<sub>2</sub>As<sub>2</sub> single crystals. Strong anisotropy between the  $a$  and  $c$  axes is revealed in our high-resolution thermal expansion measurements. The phase transition appears to be continuous, and the samples are devoid of any structural transitions over the temperature range ( $5 < T < 300$  K) of our measurements. The thermal expansion data and heat-capacity data acquired on the same samples are used to estimate the volumetric pressure derivative of  $T_c$  using the Ehrenfest relation.

Our investigation was performed on two single crystals of BaFe<sub>1.84</sub>Co<sub>0.16</sub>As<sub>2</sub> [the length and width along the measured directions for the crystals are  $4.321(1) \times 0.326(2)$  and  $4.525(1) \times 0.193(5)$  mm<sup>2</sup>]. The lattice parameters for these crystals are  $a=3.9534(7)$  Å and  $c=12.942(3)$  Å at room temperature and  $T_c=21.5$  K. Two single crystals of BaFe<sub>1.77</sub>Co<sub>0.23</sub>As<sub>2</sub> were also investigated [with length and width along the measured directions  $4.441(1) \times 0.176(2)$  and  $4.635(1) \times 0.280(5)$  mm<sup>2</sup>]. The lattice parameters for these crystal are  $a=3.9519(4)$  Å and  $c=12.937(1)$  Å at room temperature and  $T_c=16.5$  K. The crystals were grown using the FeAs flux method.<sup>5</sup> The smaller of the provided dimensions is parallel to the  $c$  axis. The Co composition was determined by microprobe analysis using an electron micro-

scope with an uncertainty of about 5%. Thermal expansion was measured using a high-resolution capacitive dilatometer cell constructed from fused quartz.<sup>12</sup> It can detect 0.1 Å changes in length for a relative resolution of about  $10^{-8}$ ; this resolution is at least 4 orders of magnitude higher than that possible with x-ray or neutron diffraction. Data are collected at an interval of 0.2 K using a warming rate of 0.20(1) K/min. The data are corrected for the empty-cell effect, measured in a separate experiment, and for the differential ex-

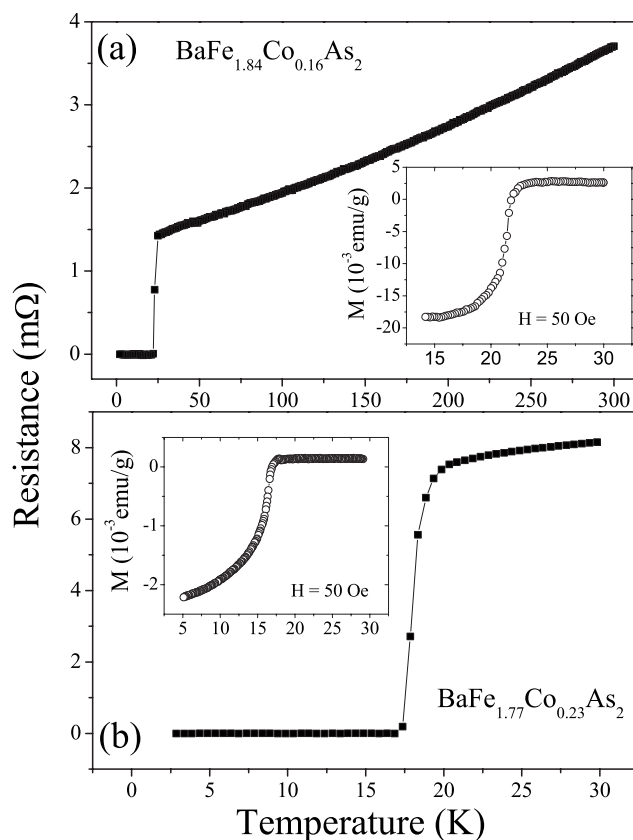


FIG. 1. Electrical resistance (main panels) and magnetization (insets) for BaFe<sub>1.84</sub>Co<sub>0.16</sub>As<sub>2</sub> (top panel) and BaFe<sub>1.77</sub>Co<sub>0.23</sub>As<sub>2</sub> (lower panel). The magnetization was measured by cooling the sample at 0.5 K/min in a constant magnetic field of 50 Oe.

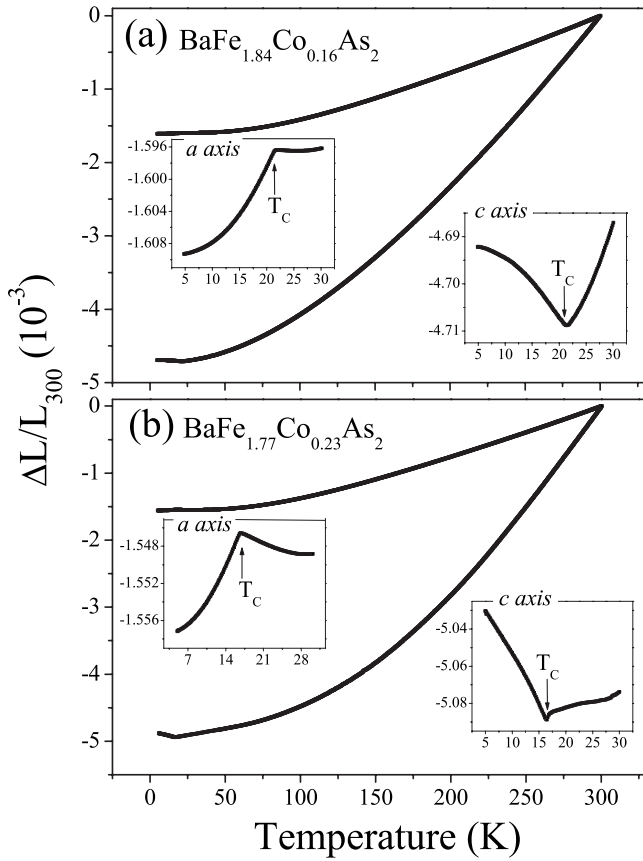


FIG. 2. Linear thermal expansion ( $\Delta L/L_{300}$ ) for the *a* (upper) and *c* (lower) axes. Insets show the region near  $T_c$ .

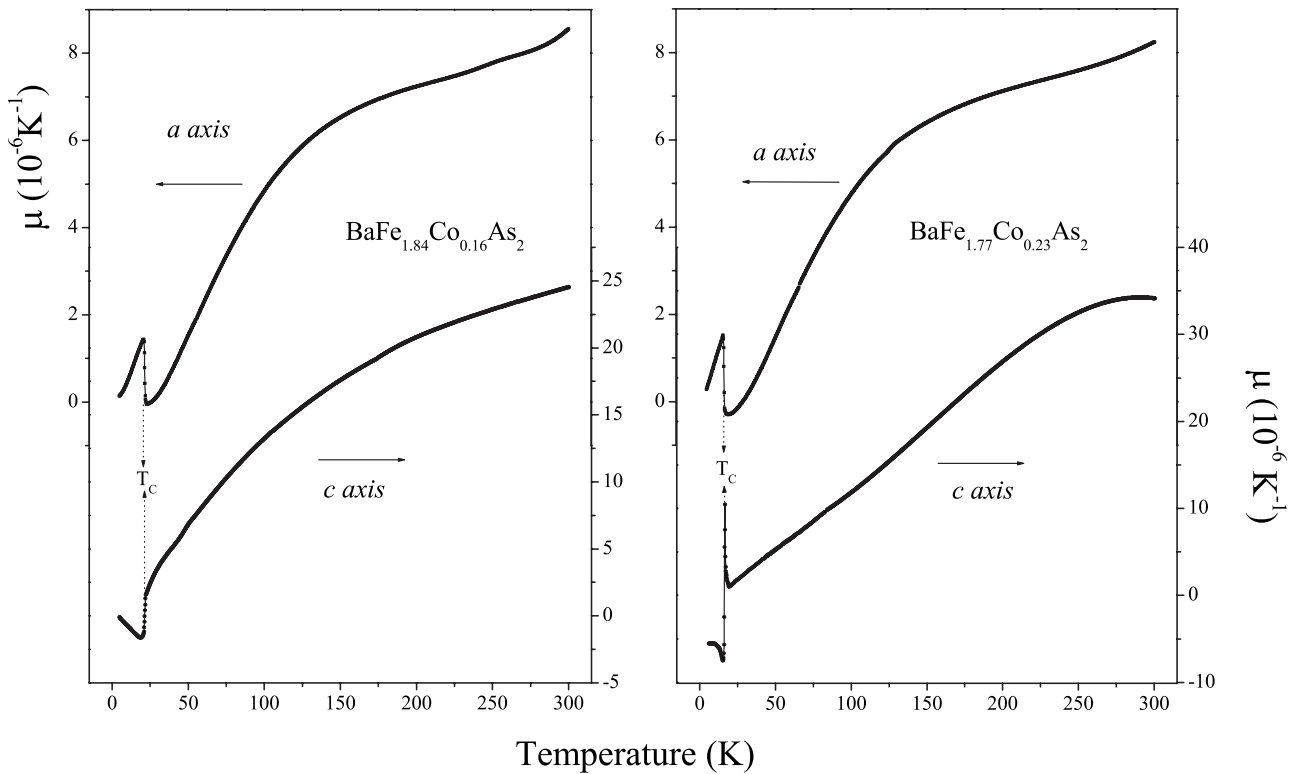


FIG. 3. Thermal expansion coefficient  $\mu = (1/L_{300} \text{ K}) \partial \Delta L / \partial T$  for the *a* and *c* axes. The left panel shows the data for  $\text{BaFe}_{1.84}\text{Co}_{0.16}\text{As}_2$  and the right panel shows the data for  $\text{BaFe}_{1.77}\text{Co}_{0.23}\text{As}_2$ .

pansion between the cell and sample.<sup>12</sup> The midpoint of the transition in the thermal expansion coefficient, a bulk thermodynamic property, was used to define  $T_c$ . Heat capacity at constant pressure  $C_p$ , dc magnetic susceptibility, and four-probe dc electrical resistivity were measured using a Quantum Design Physical Properties Measurement System.

Figure 1 shows electrical resistance (main panels) and magnetization (insets) for the two compositions investigated in this work. The current is applied perpendicular to the *c* axis, in the plane of the crystal. The magnetization was measured by cooling the sample at 0.5 K/min in a constant magnetic field of 50 Oe, which was perpendicular to the *c* axis. The obtained transition temperatures for superconductivity agree with the  $T_c$  versus composition relationship that was recently reported<sup>13,14</sup> for  $\text{Ba}(\text{Fe}_{1-x}\text{Co}_x)_2\text{As}_2$ .

Figure 2 presents the linear thermal expansion normalized to the length at 300 K,  $\Delta L/L_{300}$ , for the *a* and *c* axes of both compositions. The same behavior was observed for the second crystal of each composition. The relative changes along the *c* direction, over the entire temperature range, are about three times larger than the changes along *a*. This could be a consequence of the layered nature of  $\text{Ba}(\text{Fe}_{1-x}\text{Co}_x)_2\text{As}_2$ , with strongly covalent bonds within the layers and rather weak bonds between the layers. For both axes, the length decreases with temperature, as occurs in most materials. Along *c*,  $\Delta L/L_{300}$  increases in a dramatic fashion on cooling below  $T_c$  (see lower inset for both compositions). In the *a* direction, a distinct change in slope at  $T_c$  is also visible. The measurements in the region  $5.5 < T < 30$  K were repeated at least two times along each axis for each of the single crystals, with similar results to those shown in Fig. 2. We see no evidence

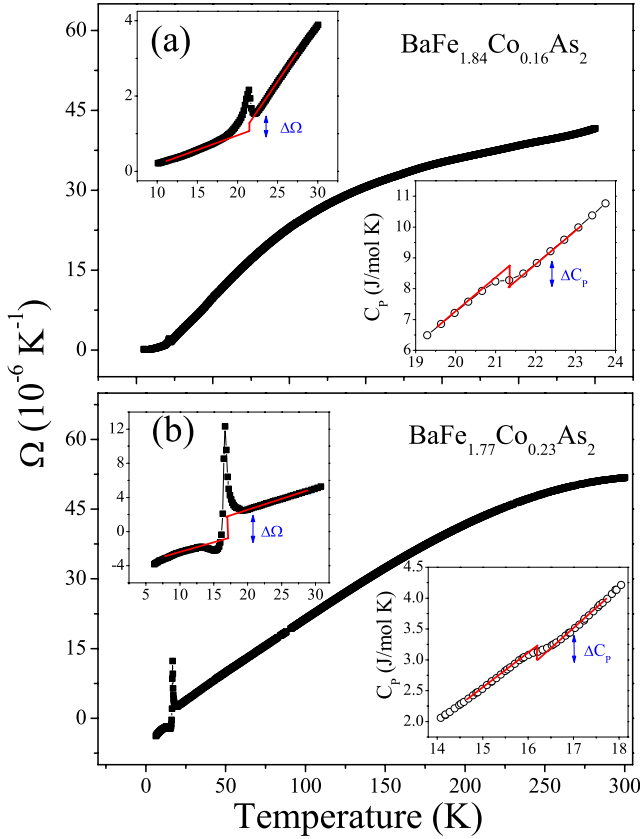


FIG. 4. (Color online) Volume thermal expansion coefficient  $\Omega$  versus  $T$  for  $\text{BaFe}_{1.84}\text{Co}_{0.16}\text{As}_2$  (upper panel) and  $\text{BaFe}_{1.77}\text{Co}_{0.23}\text{As}_2$  (lower panel). The upper insets in each panel show the region near  $T_c$ . The lower insets in each panel show the heat capacity  $C_p$  versus  $T$ . The jumps at the phase transitions are indicated by the linear lines (in red) drawn through the data.

for a structural transition in the close vicinity to  $T_c$ , which would appear as a discontinuity in  $\Delta L/L_{300}$  and would indicate a discontinuous (first-order) phase transition. It is interesting that  $\Delta L/L_{300}$  is quite large along  $c$  with a variation between 5 and 300 K that is 35% larger than that of copper,<sup>15</sup> an element with a relatively large thermal expansion.

The thermal expansion coefficient  $\mu = (1/L_{300\text{ K}}) \partial \Delta L / \partial T$  is shown in Fig. 3. In the subsequent discussion,  $\mu$  is labeled with the subscript  $i$  to denote the direction along which it was measured. We determined  $\mu_i$  by fitting the data in Fig. 2 using Chebyshev polynomials and differentiating, as reported previously.<sup>12,16</sup> This process includes cross checking with the point-by-point derivative to ascertain that no subtle features are overlooked.<sup>17</sup> In the vicinity of  $T_c$ , rather than using this fitting procedure, a point-by-point differentiation was conducted because of the sharp nature of the phase transition. Behavior similar to that shown in Fig. 3 was observed in all data collected on the crystals. As anticipated from the  $\Delta L/L_{300}$  data,  $\mu_c$  is significantly larger in magnitude than  $\mu_a$ . The jumps at  $T_c$  are clearly visible on the scale of Fig. 3; they are very anisotropic with different magnitudes and opposite signs. The general character of the data agree with some recent measurements<sup>18,19</sup> for  $\text{BaFe}_{1.84}\text{Co}_{0.16}\text{As}_2$ ,  $\text{BaFe}_{1.852}\text{Co}_{0.148}\text{As}_2$ , and  $\text{BaFe}_{1.924}\text{Co}_{0.076}\text{As}_2$ .

For a typical normal-to-superconducting phase

transition,<sup>16,20</sup> a steplike anomaly (often referred to as a jump) is expected to occur in the thermodynamic quantities  $\mu$  and heat capacity  $C_p$  (see Fig. 4) at  $T_c$ . As a result, we believe the phase transition to be continuous (i.e., second order).<sup>21</sup> The behaviors of the anomalies in  $\mu_a$  and  $\mu_c$ , where a positive jump occurs along one axis and a negative jump along the other,<sup>22</sup> are common for anisotropic superconductors. However, it is interesting that the volumetric thermal expansion coefficient  $\Omega = 2\mu_a + \mu_c$  (see Fig. 4) exhibits peaks at  $T_c$ , unlike the steplike anomaly revealed at  $T_c$  in the heat capacity (lower insets in each panel of Fig. 4). This may be associated with the large and strongly anisotropic anomalies in  $\mu_i$  at  $T_c$ , which when added undergo a partial cancellation that develops into a peak. However, a peak is also evident in  $\mu_c$  for our  $\text{BaFe}_{1.77}\text{Co}_{0.23}\text{As}_2$  sample (see Fig. 5). This leads to a larger peak in  $\Omega$  for that sample. Furthermore, a slight peak appears in the  $\Omega$  data<sup>19</sup> on  $\text{BaFe}_{1.852}\text{Co}_{0.148}\text{As}_2$ . Based on the fact that no jump is observed in  $\Delta L/L(300\text{ K})$ , within our resolution, it appears that despite the presence of this peak, our identification of the phase transition as continuous (second order) remains reasonable.

$\text{BaFe}_2\text{As}_2$  is orthorhombic below  $\sim 140$  K and tetragonal above, and this structural transition is *approximately* volume conserving.<sup>23</sup> Our data show that the extremely large first-order structural phase transition of<sup>23</sup>  $\text{BaFe}_2\text{As}_2$  is *entirely* suppressed in our Co-doped crystals. The fact that a moderate amount of Co doping, which is synonymous with electron doping,<sup>5</sup> suppresses the phase transition, suggests that the structural transition in  $\text{BaFe}_2\text{As}_2$  is a type of electronic instability. Such instabilities are not uncommon to arsenides. For example,  $\text{MnAs}$  exhibits a transition from hexagonal to orthorhombic<sup>24</sup> that is accompanied by a large volume change. Pressure can be used to tune this transition, leading to an exceptionally large magnetocaloric effect.<sup>25</sup> In analogy, quasi-hydrostatic pressure has recently been shown to suppress the structural transition in the analog compound  $\text{CaFe}_2\text{As}_2$  leading to superconductivity.<sup>7,9</sup> These comparisons underscore the fact that interesting physics often exists close to an instability.<sup>26</sup>

We now discuss some general aspects of the thermal expansion. Layered materials are known to exhibit highly anisotropic thermal expansions, as well as negative thermal expansions over some temperature ranges. This is the case in  $\text{YBa}_2\text{Cu}_3\text{O}_7$ ,  $\text{MgB}_2$ ,  $\text{Na}_x\text{CoO}_2$ , and  $\text{Li}_{0.9}\text{Mo}_6\text{O}_{17}$ .<sup>16,22,27</sup> In  $\text{MgB}_2$ , the volume thermal expansion coefficient at  $T_c$  crosses over from positive above  $T_c$  to negative below<sup>16</sup>  $T_c$ , similar to what occurs along  $c$  in  $\text{BaFe}_{1.84}\text{Co}_{0.16}\text{As}_2$  and  $\text{BaFe}_{1.77}\text{Co}_{0.23}\text{As}_2$  (see Figs. 2–5). The nature of thermal expansion has been theoretically investigated for the case of the layered material graphite,<sup>28</sup> where the thermal expansion coefficient along the  $a$  axis is small and negative, and the thermal expansion coefficient along the  $c$  axis is positive, with about twice the magnitude of that along  $a$ .<sup>29</sup> Theory attributes this to the out-of-plane vibrational frequencies that are characteristic of layered materials.<sup>28</sup> This general behavior is evident in  $\text{BaFe}_{1.84}\text{Co}_{0.16}\text{As}_2$  and  $\text{BaFe}_{1.77}\text{Co}_{0.23}\text{As}_2$ , where  $\mu_c$  is large and  $\mu_a$  is small.

Our thermal expansion and heat-capacity data can be used to calculate the pressure dependence of  $T_c$  near  $P=0$  via the Ehrenfest relation, which is given by

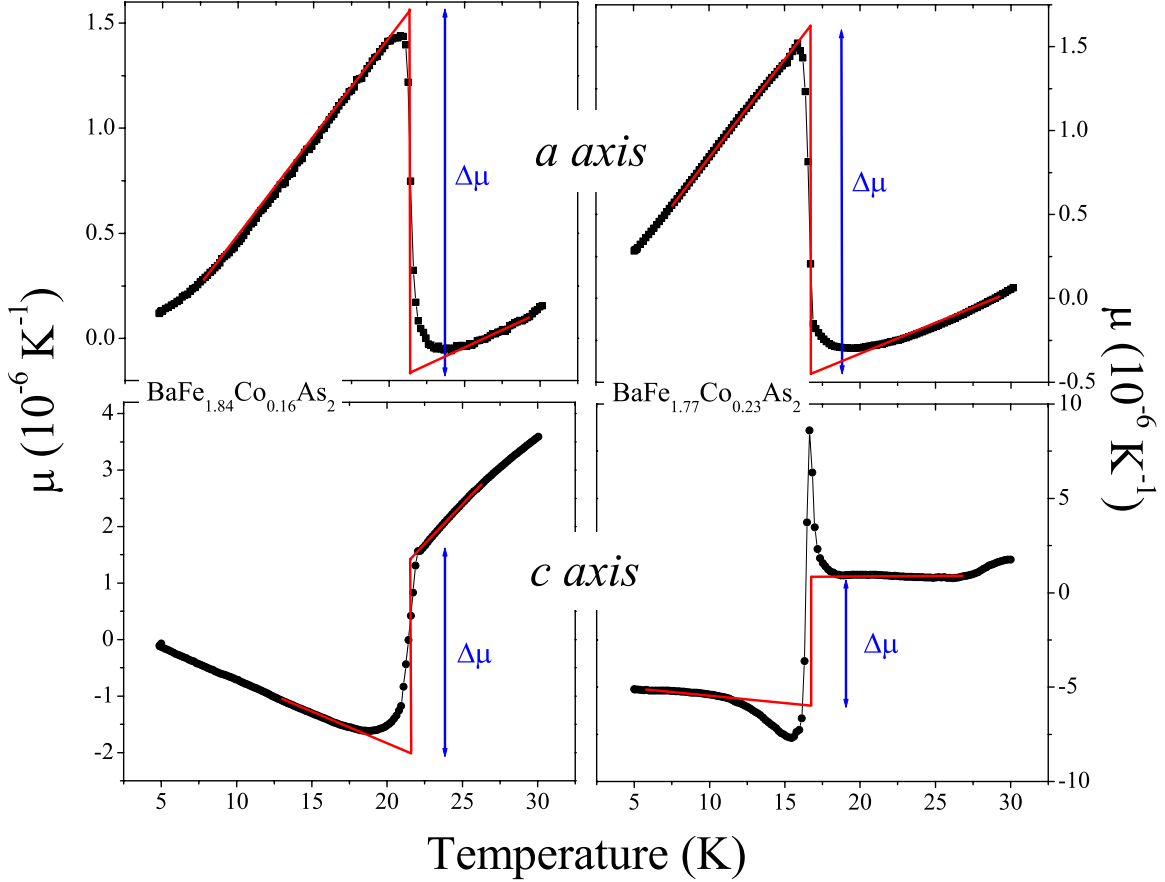


FIG. 5. (Color online) Thermal expansion coefficient  $\mu=(1/L_{300\text{ K}})\partial\Delta L/\partial T$  for the *a* and *c* axes. The left panel shows the data for  $\text{BaFe}_{1.84}\text{Co}_{0.16}\text{As}_2$  and the right panel shows the data for  $\text{BaFe}_{1.77}\text{Co}_{0.23}\text{As}_2$ . The jumps at the phase transitions are indicated by the linear lines (in red) drawn through the data.

$$\frac{dT_c}{dP} = V_m T_c \frac{\Delta\Omega}{\Delta C_P}, \quad (1)$$

where  $P$  denotes the hydrostatic pressure,  $V_m$  denotes the volume per mole, and  $\Delta C_P$  denotes the jump in the heat capacity. For this analysis, the jumps in  $\Omega$  and  $C_P$  at  $T_c$  are needed. The jumps in  $\mu_i$  are indicated by the linear lines in Fig. 5. Considering first  $\text{BaFe}_{1.84}\text{Co}_{0.16}\text{As}_2$ , after averaging the jumps, we obtained  $\Delta\mu_a = -1.5(3) \times 10^{-6}$  (an average of four measurements) and  $\Delta\mu_c = 3.6(2) \times 10^{-6}$  (an average of three measurements). As noted above, the anomalies are highly anisotropic, with opposite sign, and the jump along *c* is more than twice as large in magnitude as the jump along *a*. The jump in  $\Omega$  was calculated from  $\Delta\Omega = 2\Delta\mu_a + \Delta\mu_c$  to yield  $0.6(8) \times 10^{-6}$  (see the inset of Fig. 4 for an approximate sketch of the jump in  $\Omega$ ). From our  $C_P$  data, we extracted  $\Delta C_P = -0.471(4)$  J/mol K. As  $\text{Ba}(\text{Fe}_{1-x}\text{Co}_x)_2\text{As}_2$  crystallizes in the  $\text{ThCr}_2\text{Si}_2$  structure with 2 f.u. per unit cell,  $V_m$  was calculated to be  $6.09 \times 10^{-5}$  m<sup>3</sup>/mol. Using these values and Eq. (1), we obtained  $dT_c/dP = -1.7(2.3)$  K/GPa.

For the samples with composition  $\text{BaFe}_{1.77}\text{Co}_{0.23}\text{As}_2$  and  $T_c = 16.5$  K, we note that the kink near 27 K in the *c*-axis data of  $\text{BaFe}_{1.77}\text{Co}_{0.23}\text{As}_2$  (see Fig. 5) is associated with a slight change in the warming rate. After averaging the jumps from three measurements along each axis we obtained  $\Delta\mu_a$

$= -1.8(3) \times 10^{-6}$  (an average of four measurements),  $\Delta\mu_c = 7.2(4) \times 10^{-6}$  (an average of two measurements), and  $\Delta\Omega = 3.6(1.0) \times 10^{-6}$ . For this composition,  $\Delta\Omega$  is dominated by  $\Delta\mu_c$ . From heat-capacity measurements, we found  $\Delta C_P = -0.281(3)$  J/mol K. The calculation using these values,  $V_m = 6.08 \times 10^{-5}$  m<sup>3</sup>/mol and Eq. (1), yields  $dT_c/dP = -13(4)$  K/GPa. By comparing the  $dT_c/dP$  values for the two compositions, it seems reasonable to conclude that  $\Delta\Omega$  is dominated by  $\Delta\mu_c$  in  $\text{BaFe}_{1.77}\text{Co}_{0.23}\text{As}_2$  and that this is an important contributor to the large negative  $dT_c/dP$ .

Measurements of electrical resistivity under pressure<sup>30,31</sup> on  $\text{Ba}(\text{Fe}_{1-x}\text{Co}_x)_2\text{As}_2$  for  $0 < x < 0.1$  revealed values ranging from  $dT_c/dP = 4.3$  K/GPa for  $x = 0.02$  to  $dT_c/dP < 1$  K/GPa for  $x = 0.099$ . A maximum value of  $dT_c/dP = 0.65$  K/GPa was observed for  $\text{BaFe}_{1.92}\text{Co}_{0.08}\text{As}_2$ . Thermal expansion measurements and the Ehrenfest analysis found<sup>18</sup>  $dT_c/dP = -0.9(3)$  K/GPa for  $\text{BaFe}_{1.84}\text{Co}_{0.16}\text{As}_2$ ,  $dT_c/dP = -6.1$  K/GPa for  $\text{BaFe}_{1.924}\text{Co}_{0.076}\text{As}_2$ , and  $dT_c/dP = -1.8$  K/GPa for  $\text{BaFe}_{1.852}\text{Co}_{0.148}\text{As}_2$ .<sup>19</sup> A plot of  $dT_c/dP$  versus Co composition (not shown) using the  $dT_c/dP$  values determined from thermal expansion measurements (including those herein) reveals no clear trend, whereas a peak in  $dT_c/dP$  versus  $x$  is evident in the values determined by electrical resistivity.<sup>31</sup> Most notable is the fact that the  $dT_c/dP$  determined using analyses similar to ours reveals  $dT_c/dP < 0$  while direct measurement reveals  $dT_c/dP > 0$ . However,

it has recently been pointed out that nonhydrostatic pressure conditions can lead to very different results in  $\text{CaFe}_2\text{As}_2$ , which exhibits superconductivity under nonhydrostatic conditions<sup>7</sup> and no superconductivity under hydrostatic conditions using helium as a pressure transmitting medium.<sup>32</sup> Thus, it may be prudent to wait for more measurements to establish the source of the disagreement between  $dT_c/dP$  determined under nonhydrostatic conditions<sup>30,31</sup> and  $dT_c/dP$  determined from thermodynamic analysis of thermal expansion data (equivalent to hydrostatic conditions).<sup>18,19</sup>

$T_c$  increases with pressure in  $\text{La}(\text{O}_{1-y}\text{F}_y)\text{FeAs}$  ( $y=0.11$ ) at a rate of  $dT_c/dP=1.2$  K/GPa.<sup>33</sup> In the case of  $\text{SmFeAsO}_{1-y}\text{F}_y$  ( $y=0.3$ ) and  $\text{Ba}_{0.55}\text{K}_{0.45}\text{Fe}_2\text{As}_2$ ,  $T_c$  decreases at rates of  $dT_c/dP=-2.3$  K/GPa and  $dT_c/dP=-1.5$  K/GPa, respectively.<sup>34,35</sup> It has recently been shown that the sign of  $dT_c/dP$  depends on the doping level<sup>34,36</sup> and that  $T_c$  varies with carrier concentration in a parabolic manner for some As-based superconductors.<sup>34</sup> In cuprate superconductors, the parabolic behavior of  $T_c$  versus carrier concentration is responsible for the systematic occurrence<sup>37</sup> of positive and negative values of  $dT_c/dP$ . Presumably, similar physics is at play in the FeAs superconductors.

Finally, it has become fairly common to estimate uniaxial pressure derivatives<sup>22</sup> using the jumps in  $\mu_i$  and  $C_p$ . This analysis was recently conducted<sup>18,19</sup> using anisotropic thermal expansion data on  $\text{Ba}(\text{Fe}_{1-x}\text{Co}_x)_2\text{As}_2$ . Its use is based on an argument of Testardi,<sup>38</sup> which neglects the off-diagonal elements of the stress tensor<sup>39</sup> in calculating  $dT_c/dP$ . For

example, if uniaxial pressure were applied along  $c$ , according to the Poisson effect, the crystal must expand along the two perpendicular directions. This fact is neglected in the uniaxial Ehrenfest relation that is commonly used.<sup>18,19,22</sup> For this reason, we have not produced such an analysis. A detailed theoretical description of this is in preparation.<sup>40</sup>

In summary, our results reveal the anisotropic thermal expansion of  $\text{Ba}(\text{Fe}_{1-x}\text{Co}_x)_2\text{As}_2$ . The  $c$ -axis expansion is about three times larger than the  $a$ -axis expansion. Furthermore, the  $c$ -axis expansion is very large with a value for  $\mu$  that is about 35% larger than copper, an element with a large thermal expansion coefficient. The anomalies at  $T_c$  suggest that the normal-superconducting phase transition is continuous (i.e., second order). The orthorhombic to tetragonal phase transition that is observed in  $\text{BaFe}_2\text{As}_2$  is completely absent in the two compositions that were measured. Finally, the Ehrenfest relation was applied to estimate the volumetric pressure derivatives of  $T_c$  for both compositions.

This material is based on the work supported by the U.S. Department of Energy (Contract No. DE-FG02-07ER46269) and the National Science Foundation (Contract No. DMR-0504769). Research at ORNL was sponsored by the Division of Materials Sciences and Engineering, Office of Basic Energy Sciences, U.S. Department of Energy. Discussions with A. de Campos, A. B. Vorontsov, B. D. White, and Y.-K. Yu are greatly appreciated.

- 
- <sup>1</sup>Y. Kamihara, T. Watanabe, M. Hirano, and H. Hosono, *J. Am. Chem. Soc.* **130**, 3296 (2008); G. F. Chen, Z. Li, D. Wu, G. Li, W. Z. Hu, J. Dong, P. Zheng, J. L. Luo, and N. L. Wang, *Phys. Rev. Lett.* **100**, 247002 (2008); H. Takahashi, K. Igawa, K. Arii, Y. Kamihara, M. Hirano, and H. Hosono, *Nature (London)* **453**, 376 (2008); H. Kito, H. Eisakt, and A. Iyo, *J. Phys. Soc. Jpn.* **77**, 063707 (2008).
- <sup>2</sup>M. Rotter, M. Tegel, and D. Johrendt, *Phys. Rev. Lett.* **101**, 107006 (2008).
- <sup>3</sup>G. F. Chen, Z. Li, G. Li, W. Z. Hu, J. Dong, J. Zhou, X. D. Zhang, P. Zheng, N. L. Wang, and J. L. Luo, *Chin. Phys. Lett.* **25**, 3403 (2008).
- <sup>4</sup>K. Sasmal, B. Lv, B. Lorenz, A. M. Guloy, F. Chen, Y. Y. Xue, and C. W. Chu, *Phys. Rev. Lett.* **101**, 107007 (2008).
- <sup>5</sup>A. S. Sefat, R. Jin, M. A. McGuire, B. C. Sales, D. J. Singh, and D. Mandrus, *Phys. Rev. Lett.* **101**, 117004 (2008).
- <sup>6</sup>T. Park, E. Park, H. Lee, T. Klimczuk, E. D. Bauer, F. Ronning, and J. D. Thompson, *J. Phys.: Condens. Matter* **20**, 322204 (2008).
- <sup>7</sup>M. S. Torikachvili, S. L. Bud'ko, N. Ni, and P. C. Canfield, *Phys. Rev. Lett.* **101**, 057006 (2008).
- <sup>8</sup>P. L. Alireza, Y. T. C. Ko, J. Gollet, C. M. Petrone, J. M. Cole, G. G. Lonzarich, and S. E. Sebastian, *J. Phys.: Condens. Matter* **21**, 012208 (2009).
- <sup>9</sup>W. Yu, A. A. Aczel, T. J. Williams, S. L. Bud'ko, N. Ni, P. C. Canfield, and G. M. Luke, *Phys. Rev. B* **79**, 020511(R) (2009).
- <sup>10</sup>M. Rotter, M. Tegel, D. Johrendt, I. Schellenberg, W. Hermes, and R. Pöttgen, *Phys. Rev. B* **78**, 020503(R) (2008).
- <sup>11</sup>M. Tegel, M. Rotter, V. Weiß, F. M. Schappacher, R. Pöttgen, and D. Johrendt, *J. Phys.: Condens. Matter* **20**, 452201 (2008).
- <sup>12</sup>J. J. Neumeier, R. K. Bollinger, G. E. Timmins, C. R. Lane, R. D. Krogstad, and J. Macaluso, *Rev. Sci. Instrum.* **79**, 033903 (2008).
- <sup>13</sup>F. Ning, K. Ahilan, T. Imai, A. S. Sefat, R. Jin, M. A. McGuire, B. C. Sales, and D. Mandrus, *J. Phys. Soc. Jpn.* **78**, 013711 (2009).
- <sup>14</sup>J.-H. Chu, J. G. Analytis, C. Kucharczyk, and I. R. Fisher, *Phys. Rev. B* **79**, 014506 (2009).
- <sup>15</sup>F. R. Kroeger and C. A. Swenson, *J. Appl. Phys.* **48**, 853 (1977).
- <sup>16</sup>J. J. Neumeier, T. Tomita, M. Debessai, J. S. Schilling, P. W. Barnes, D. G. Hinks, and J. D. Jorgensen, *Phys. Rev. B* **72**, 220505(R) (2005).
- <sup>17</sup>The capacitance channel has a resolution of 1 part in  $10^8$  while the temperature channel has a resolution of 1 part in  $10^5$ . This, and the close spacing between data points, leads to scatter in the derivative of  $\Delta L/L_{300}$ . Our fitting procedure minimizes this scatter.
- <sup>18</sup>F. Hardy, P. Adelman, T. Wolf, H. v. Löhneysen, and C. Meingast, *Phys. Rev. Lett.* **102**, 187004 (2009).
- <sup>19</sup>S. L. Bud'ko, N. Ni, S. Nandi, G. M. Schmiedeshoff, and P. C. Canfield, *Phys. Rev. B* **79**, 054525 (2009).
- <sup>20</sup>J. A. Souza, Y.-K. Yu, J. J. Neumeier, H. Terashita, and R. F. Jardim, *Phys. Rev. Lett.* **94**, 207209 (2005).

- <sup>21</sup>The phase transition was measured via electrical resistance by warming and cooling through  $T_c$  at a rate of 0.2 K/min. The two curves agreed within 0.01 K.
- <sup>22</sup>V. Pasler, P. Schweiss, C. Meingast, B. Obst, H. Wühl, A. I. Rykov, and S. Tajima, *Phys. Rev. Lett.* **81**, 1094 (1998).
- <sup>23</sup>N. Ni, S. L. Bud'ko, A. Kreyssig, S. Nandi, G. E. Rustan, A. I. Goldman, S. Gupta, J. D. Corbett, A. Kracher, and P. C. Canfield, *Phys. Rev. B* **78**, 014507 (2008).
- <sup>24</sup>L. M. Sandratskii and E. Şaşıoğlu, *Phys. Rev. B* **74**, 214422 (2006), and references therein.
- <sup>25</sup>S. Gama, A. A. Coelho, A. de Campos, A. M. G. Carvalho, F. C. G. Gandra, P. J. von Ranke, and N. A. de Oliveira, *Phys. Rev. Lett.* **93**, 237202 (2004).
- <sup>26</sup>S. A. Kivelson, G. Aeppli, and V. J. Emery, *Proc. Natl. Acad. Sci. U.S.A.* **98**, 11903 (2001).
- <sup>27</sup>C. A. M. dos Santos, J. J. Neumeier, Y.-K. Yu, R. K. Bollinger, R. Jin, D. Mandrus, and B. C. Sales, *Phys. Rev. B* **74**, 132402 (2006); C. A. M. dos Santos, B. D. White, Y.-K. Yu, J. J. Neumeier, and J. A. Souza, *Phys. Rev. Lett.* **98**, 266405 (2007).
- <sup>28</sup>R. A. Suleimanov and N. A. Abdullaev, *Carbon* **31**, 1011 (1993); N. A. Abdullaev, *Phys. Solid State* **43**, 727 (2001).
- <sup>29</sup>A. C. Bailey and B. Yates, *J. Appl. Phys.* **41**, 5088 (1970).
- <sup>30</sup>K. Ahilan, J. Balasubramaniam, F. L. Ning, T. Imai, A. S. Sefat, R. Jin, M. A. McGuire, B. C. Sales, and D. Mandrus, *J. Phys.: Condens. Matter* **20**, 472201 (2008).
- <sup>31</sup>K. Ahilan, F. L. Ning, T. Imai, A. S. Sefat, M. A. McGuire, B. C. Sales, and D. Mandrus, arXiv:0904.2215 (unpublished).
- <sup>32</sup>D. K. Pratt, Y. Zhao, S. A. J. Kimber, A. Hiess, D. N. Argyriou, C. Broholm, A. Kreyssig, S. Nandi, S. L. Budko, N. Ni, P. C. Canfield, R. J. McQueeney, and A. I. Goldman, *Phys. Rev. B* **79**, 060510(R) (2009).
- <sup>33</sup>W. Lu, J. Yang, X. L. Dong, Z. A. Ren, G. C. Che, and Z. X. Zhao, *New J. Phys.* **10**, 063026 (2008).
- <sup>34</sup>B. Lorenz, K. Sasmal, R. P. Chaudhury, X. H. Chen, R. H. Liu, T. Wu, and C. W. Chu, *Phys. Rev. B* **78**, 012505 (2008).
- <sup>35</sup>M. S. Torikachvili, S. L. Bud'ko, N. Ni, and P. C. Canfield, *Phys. Rev. B* **78**, 104527 (2008).
- <sup>36</sup>M. Gooch, B. Lv, B. Lorenz, A. M. Guloy, and C. W. Chu, *Phys. Rev. B* **78**, 180508(R) (2008).
- <sup>37</sup>J. J. Neumeier and H. A. Zimmermann, *Phys. Rev. B* **47**, 8385 (1993).
- <sup>38</sup>L. R. Testardi, *Phys. Rev. B* **12**, 3849 (1975).
- <sup>39</sup>L. D. Landau and E. M. Lifshitz, *Theory of Elasticity* (Pergamon, London, 1959), p. 6.
- <sup>40</sup>Y.-K. Yu and J. J. Neumeier (unpublished).